Supplemental data

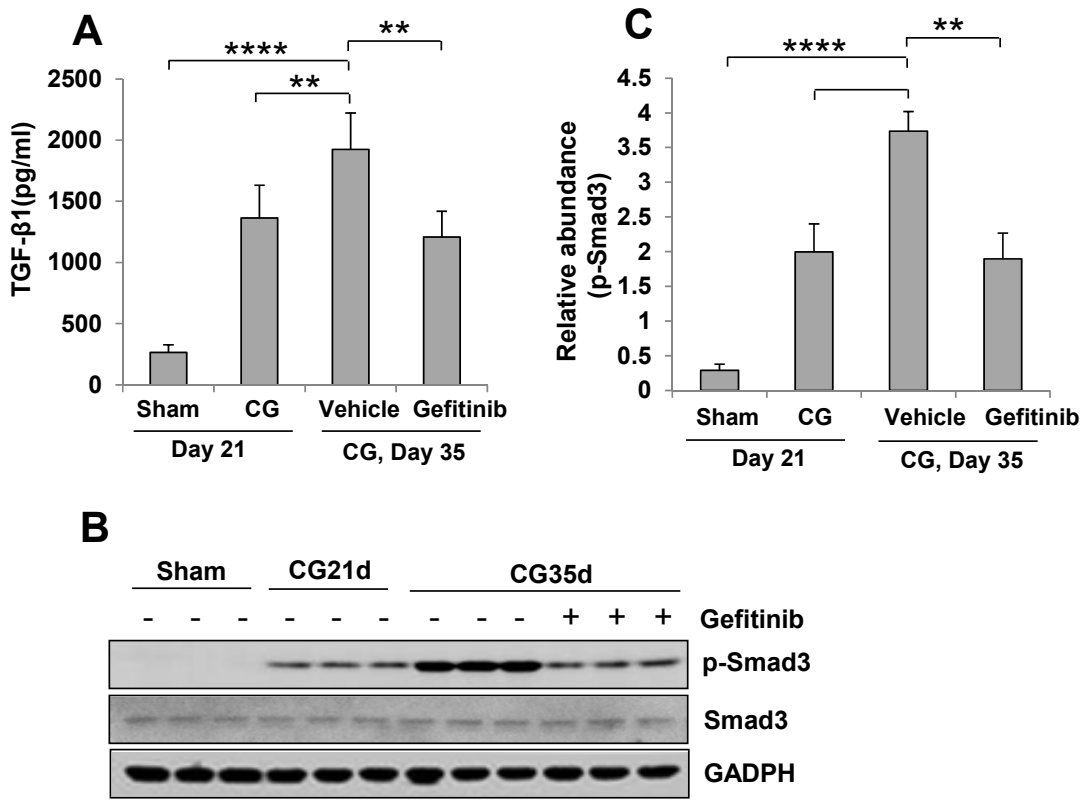

Figure 1S. Delayed gefitinib administration inhibits production of TGF-β1 and activation of Smad3in the peritoneum after CG injury. Experimental design was the same as indicated in Figure 10A. (A) The expression level of TGF-β1 was measured by ELISA. (B) Peritoneum tissue lysates were subjected to immunoblot analysis with specific antibodies against p-Smad3, Smad3 or GAPDH. (C) Expression level of p-Smad3 was quantified by densitometry and normalized with Smad3. Data are means ± S.E.M. (n = 6). Means with different superscript letters are significantly different from one another ($P < 0.05$).

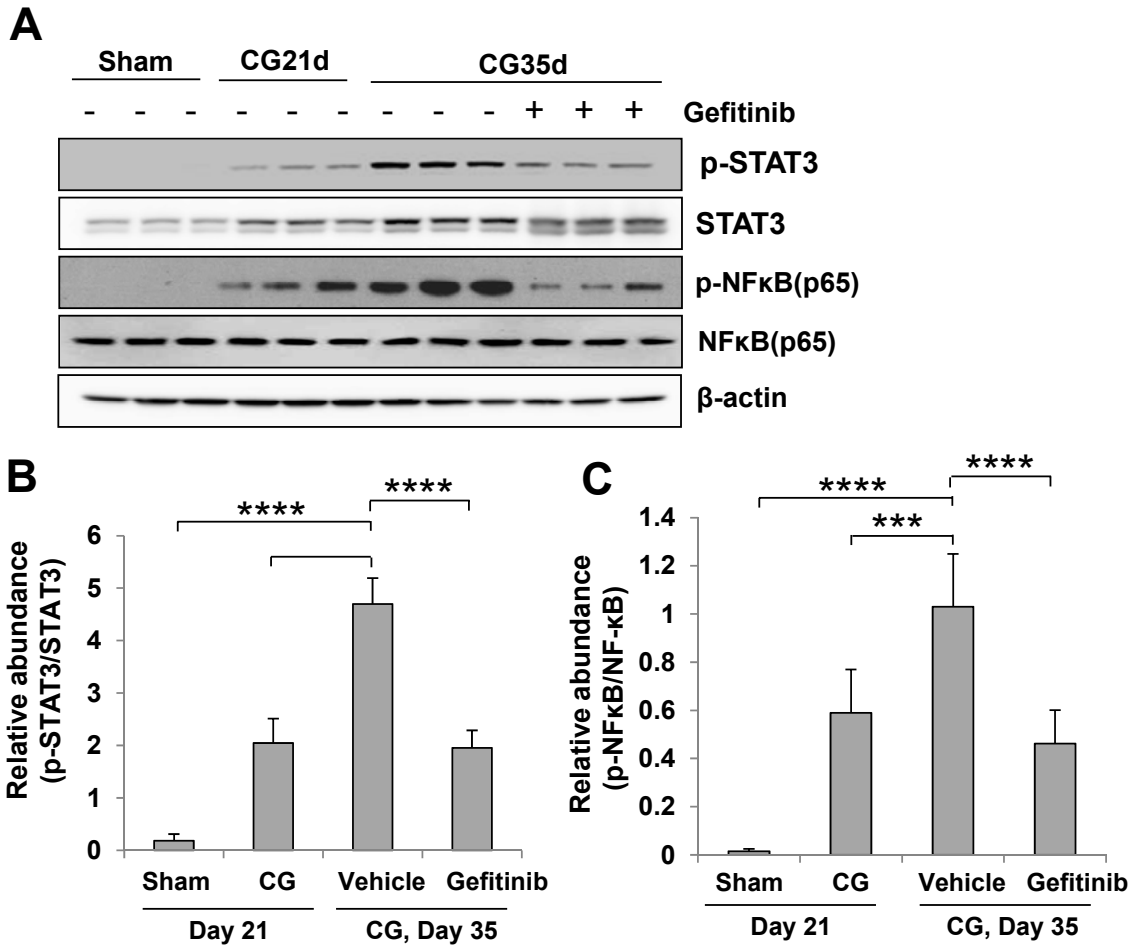

Figure 2S. Delayed gefitinib administration inhibits phosphorylation of STAT3 and NF-κB(p65) in the peritoneum after CG injury. Experimental design was the same as indicated in Figure 10A. **(**A)Peritoneal tissue lysates were subjected to immunoblot analysis with specific antibodies against p-STAT3, STAT3, p-NF-κB(p65), NF-κB(p65) or β-actin. (B) Expression level of p-STAT3 was quantified by densitometry and normalized with STAT3. (C) Expression level of p-NF-κB(p65) was quantified by densitometry and normalized with NF-κB(p65). Data are means ± S.E.M. (n = 6). Means with different superscript letters are significantly different from one another ($P < 0.05$).

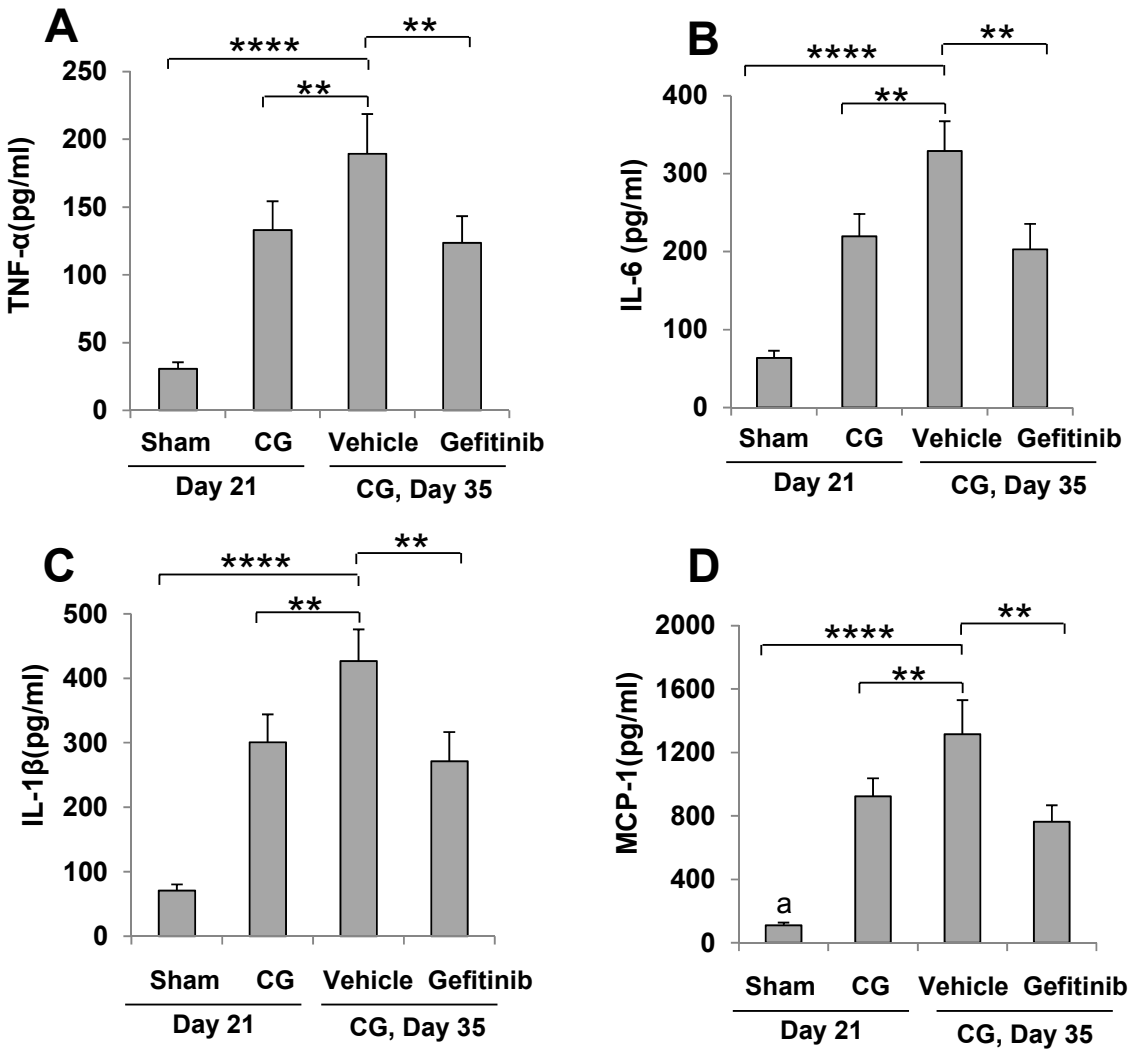

Figure 3S. Delayed gefitinib administration inhibits CG-induced production of multiple inflammatory cytokines in peritoneal fibrosis. Experimental design was the same as indicated in Figure 10A. Graphs show the expression level of TNF-α (A), IL-6 (B), IL-1β (C), and MCP-1 (D) by ELISA. Data are means ± S.E.M. (n = 6). Means with different superscript letters are significantly different from one another ($P < 0.05$).

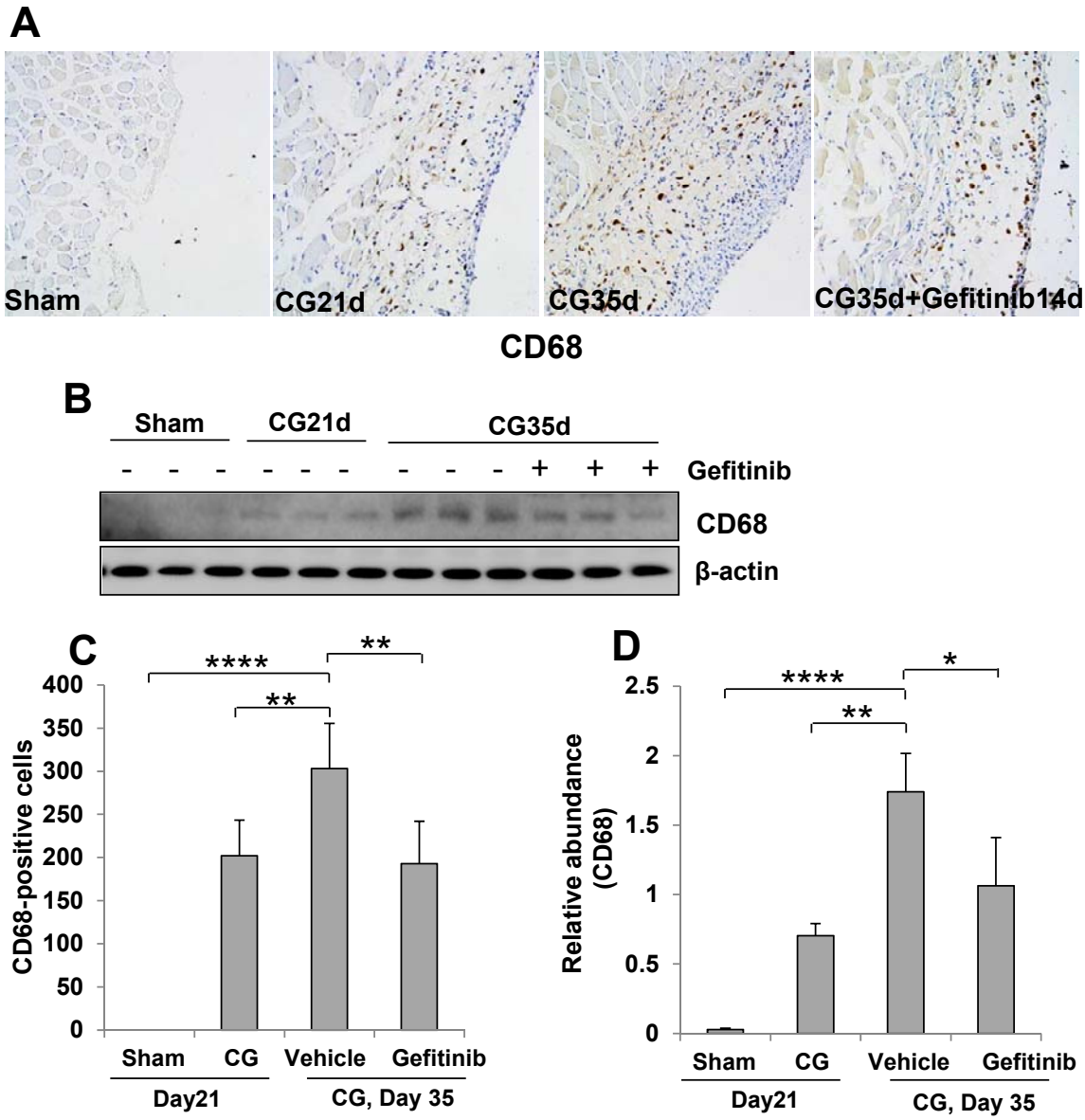

Figure4S. Delayed gefitinib administration blocks infiltration of macrophages to peritoneum after CG injury. Experimental design was the same as indicated in Figure 10A. (A)Photomicrographs illustrate immunohistochemical staining of CD68 in the submesothelial compact zone. (B)Peritoneum tissue lysates were subjected to immunoblot analysis with specific antibodies against CD68 or β-actin. (C) Graph shows the number of CD68-postive cells. (D)Expression level of CD68 was quantified by densitometry and normalized with β-actin. Data are means ± S.E.M. (n = 6). Means with different superscript letters are significantly different from one another ($P < 0.05$).

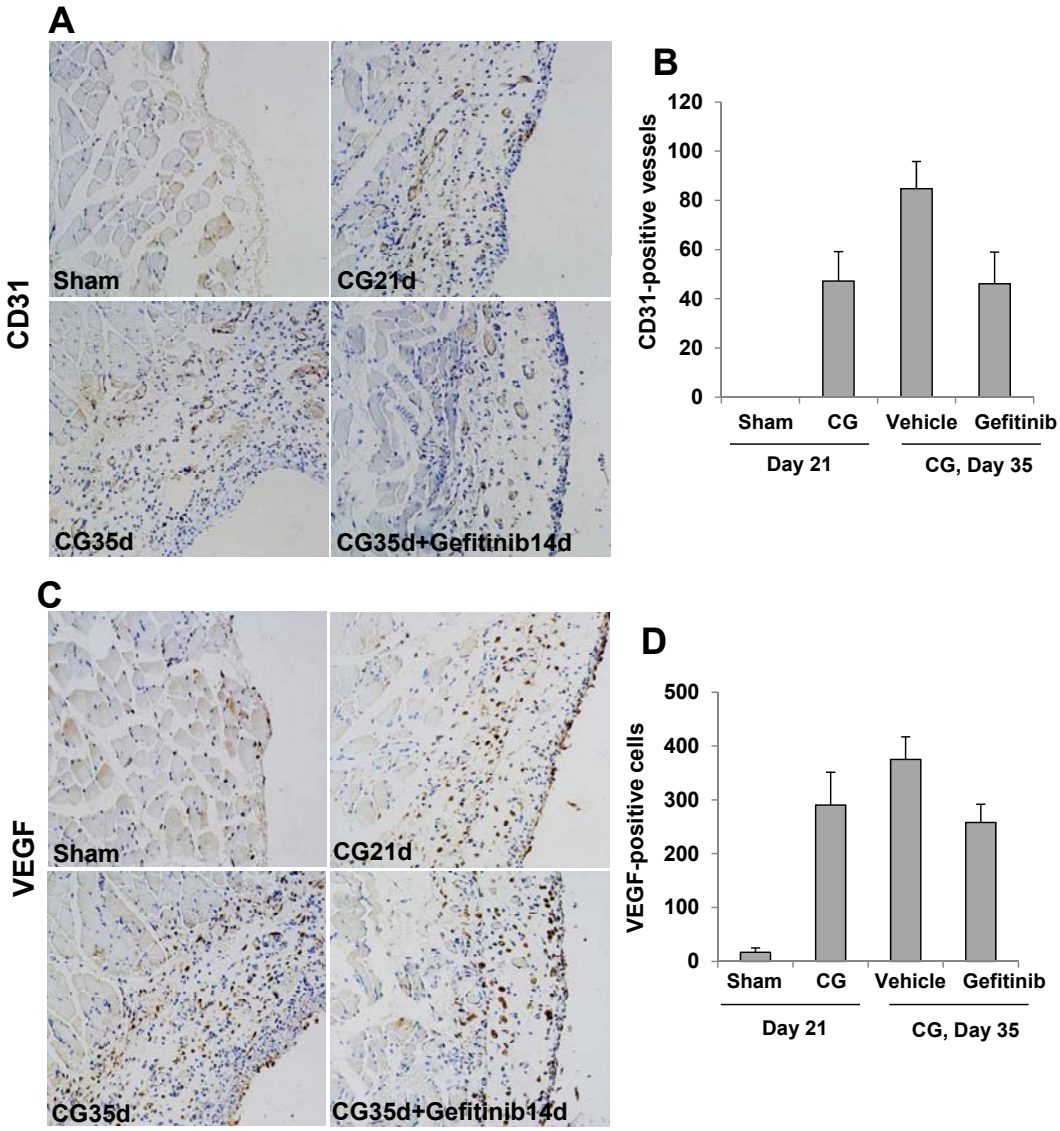

Figure 5S. Delayed gefitinib administration inhibits on CG-induced expression of CD31 andVEGF in the peritoneum. Experimental design was the same as indicated in Figure 10A.Photomicrographs illustrate immunohistochemical staining of CD31 **(**A)or VEGF (C) in the submesothelial compact zone. (B) Graph shows the number of CD31-postive vessels. (D) Graph shows the numberof VEGF-positive cells from 10 random fields (200×) (means ± S.E.M.). Data are means ± S.E.M. (n = 6). Means with different superscript letters are significantly different from one another ($P < 0.05$).

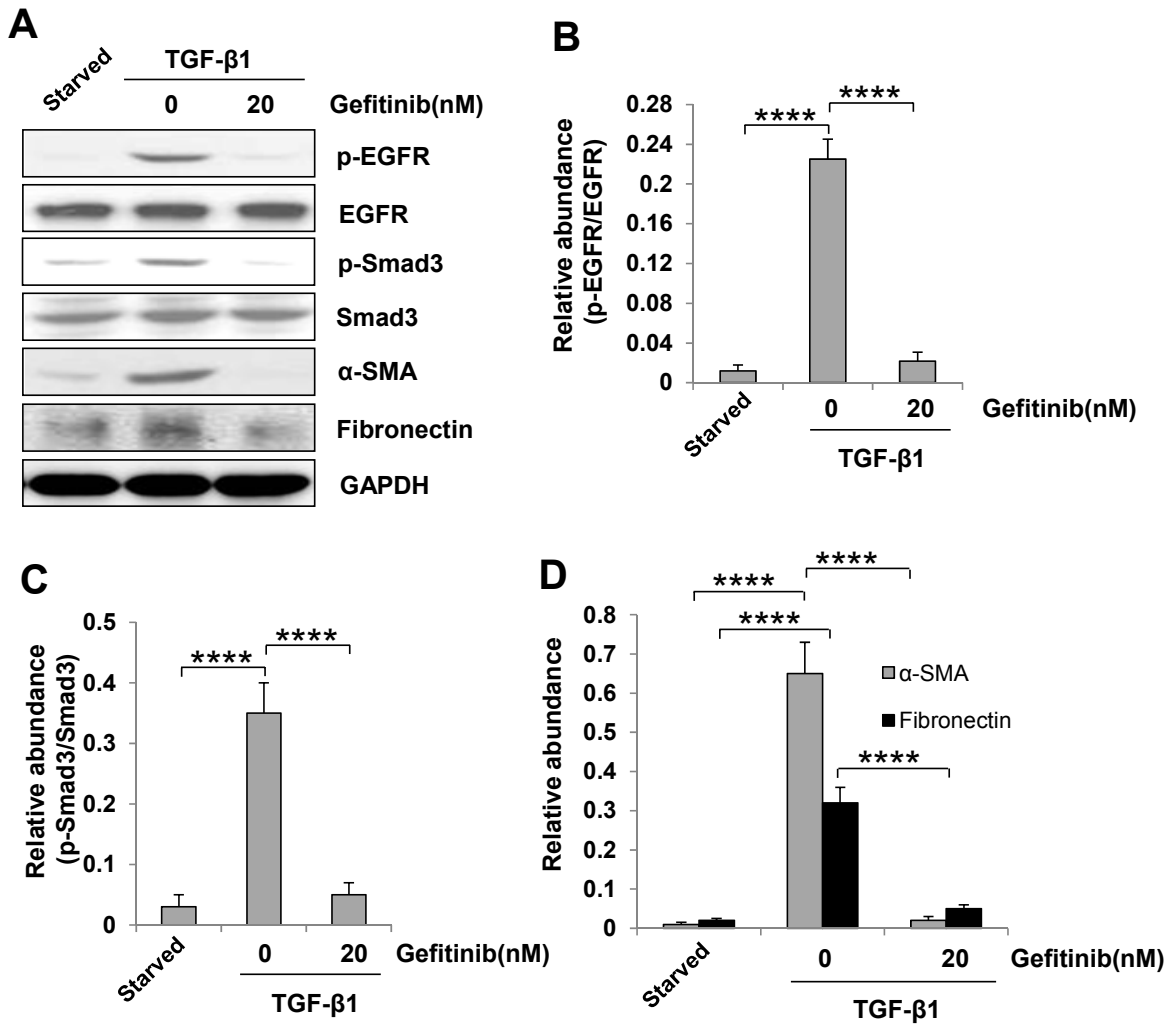

Figure 6S. EGFR mediates TGF-β induced epithelial-to-mesenchymal transition of peritoneal mesothelium cells. Human peritoneal mesothelium cells (HPMCs) were starved for 24 hour with DMEM medium containing 0.5% FBS and then exposed to 1 ng/ml TGF-β1 foran additional 24 hours in the absence or presence of 20 ng/ml gefitinib. Cells were harvested and cell lysates were subjected to the immunoblot analysis with antibodies against phospho-EGFR (EGFR), EGFR, phospho-SMAD3 (p-SMAD3), α-SMA, Febronectin, or GAPDH (A). Expression level of p-EGFR and p-Smad3 was quantified by densitometry, and p-EGFR was normalized with EGFR (N) and p-Smad3 was normalized withSmad3 (C). Expression levels of type I collagen (G), and α-SMA (H) were quantified by densitometry and normalized with GAPDH, respectively (D). Data are means ± SEM (n =6). NS (no significance), **P<0.01 versus sham controls or TGF-β1 + vehicle as indicated.